

Destruction of attractive bosonic cloud due to high spatial coherence in tight trap

Anindya Biswas¹, Barnali Chakrabarti^{2,3}, Tapan Kumar Das¹ and Luca Salasnich⁴

¹ *Department of Physics, University of Calcutta, 92 A.P.C. Road, Kolkata 700009, India.*

² *Instituto de Física, Universidade of São Paulo, CP 66318, 05315-970, São Paulo, Brazil.*

³ *Department of Physics, Lady Brabourne College,
P1/2 Surawardi Avenue, Kolkata 700017, India.*

⁴ *Dipartimento di Fisica "Galileo Galilei" and CNISM,
Università di Padova, Via Marzolo 8, 35122 Padova, Italy.*

We study coherence of trapped bosonic cloud with attractive finite-range interaction in a tight harmonic trap. One-body density and pair distribution function in the ground state for different trap sizes are calculated. We also calculate healing length and the correlation length which signify the presence of high spatial coherence in a very tight trap leading to the destruction of the condensate for a fixed particle number. This is in marked variance with the usual collapse of the attractive metastable condensate when $N > N_{cr}$. Thus we investigate the critical frequency and critical size of the trap for the existence of attractive BEC. The finite range interaction gives a nonlocal effect in the effective many-body potential and we observe a high-density stable branch besides the known metastable branch. Moreover, the new branch shows universal behavior even in the very tight trap.

PACS numbers: 03.75.Hh, 03.65.Ge, 03.75.Nt

Keywords: Bose-Einstein condensate, Attractive interaction, Potential Harmonics method

I. INTRODUCTION

Trapped ultracold bosonic atoms have attracted a revival of interest since the achievement of the Bose Einstein condensate of dilute gases. The standard defining property of Bose-Einstein condensation (BEC) is the macroscopic occupation of the single particle ground state for the ideal system. In the case of an interacting system, BEC is often related to the off-diagonal long-range order [1, 2]. By controlling the external magnetic field, one can virtually manipulate the interatomic force as well as the trap size. This can change the situation from a weakly interacting case to a very strongly interacting one and obviously the role of interatomic correlations come in the picture. Experimental relevance stems from the fact that experiments designed to produce the interference pattern in BEC are closely related with the study of coherence properties.

We investigate a weakly interacting Bose gas in the presence of an external trap. We consider a finite number of bosons interacting via the finite range van der Waals interaction, instead of the commonly used zero-range contact interaction. The $-\frac{C_6}{r^6}$ tail introduces an attractive non local interaction. ^7Li is particularly interesting due to its negative scattering length and when the number of bosons is below some threshold value, a metastable condensate appears. Due to the attractive interaction, the effect of correlation becomes important even in the weakly interacting gas and we expect to get new physics in the study of correlation properties. Although it is commonly believed that the Gross-Pitaevskii (GP) equation, based on a mean-field approach and a contact interaction, is adequate for weakly interacting Bose gases, but in the present study we utilize an approximate many-body technique which

is more rigorous and retains all possible two-body correlations [3–5]. This technique, called correlated potential harmonics (CPH) method, uses a subset of full hyperspherical harmonics (HH) expansion basis. While the latter is exact and incorporates all correlations in the many-body wave function, CPH basis retains only two-body correlations and ignores higher-body correlations. This assumption is manifestly valid in a typical laboratory BEC, which must be extremely dilute to avoid depletion due to recombination through three-body collisions. The HH method is very cumbersome and is practicable only for three-body systems. But in the CPH method, the bulk of superfluous basis functions are eliminated, so that it can be adopted for a large number of bosons (see Sec. II for details). It has been successfully applied to attractive BECs and repulsive systems containing up to 14000 particles [4, 5]. The method is important especially in the study of correlation properties in realistic condensates. Thus the motivation of our present work is as follows. Firstly, to study different correlation properties in the ground state, like one-body density and pair-distribution function for few hundred ^7Li atoms in the external three-dimensional trap. This facilitates the investigation of the effect of interatomic correlations in the many-body wave function on the bulk correlation properties of the condensate. To quantify the latter, we also calculate the healing length which is another key quantity in the study of coherence properties. Secondly, we investigate the effect of the change of trap size on the correlation properties. By controlling the trap frequency it is possible to make tighter traps. We observe that in a tighter trap the metastable condensate becomes highly correlated. Effective correlation length and the healing length reduce drastically, as the trap size decreases; however, they remain larger than the trap size, indicating strong bulk

spatial correlation within the metastable condensate. In addition to the metastable condensate, the many-body system exhibits a strongly attractive narrow well, which supports cluster states (see below). Below a critical trap size the metastable region in the effective many-body potential disappears. This manifests the destruction of a metastable condensate in a very tight trap. We estimate the critical trap size above which BEC can be observed. The disappearance of the condensate in a very tight trap significantly differs from the usual collapse of attractive BEC in a large trap.

Due to the presence of a realistic interaction with a strong repulsive core, we have a deep but finite attractive well outside a repulsive core on the left side of the metastable region in the effective potential. Hence, besides the appearance of the low density metastable BEC, we also find a stable branch at high density which leads to the formation of atomic clusters. With decreasing trap size, the metastable branch shrinks and eventually disappears (resulting in a collapse due to squeezing). However the attractive well of the effective potential supporting the high density branch remains invariant in position, magnitude and shape with decrease in trap size. Thus it exhibits a universal behavior. The energy and size of the cluster do not change with the trap size. In earlier calculations [6–8], a non-local effective interaction in the momentum space, which is equivalent to a local repulsive contact interaction plus a finite-range attractive interaction in the coordinate space was adopted in a variational calculation of the GP equation. This also produced the narrow attractive well and the associated high-density branch, in addition to the low-density metastable branch. On the other hand, a purely attractive local contact interaction in the GP equation produces a pathological essential singularity at the origin, besides the metastable region. In Ref. [6, 7], quantum tunneling rates between the low- and high-density branches and the decay rates due to two- and three-body collisions were reported. Nature of transitions between the two branches as a function of the number of bosons was also investigated. In the present study, we obtain these two branches as a result of using the realistic van der Waals interaction having a strong short-range repulsion (due to nucleus-nucleus repulsion) and a long-range attraction, in an approximate many-body theory, which incorporates all two-body correlations. We focus on the correlation properties and investigate the effect of decreasing trap size.

The paper is organized as follows. The many-body calculation technique is presented in Sec.II. Sec.III presents the calculation of many-body effective potential and different correlation properties like one-body density and pair distribution function. Sec.IV contains a summary and the conclusions.

II. MANY-BODY CALCULATION WITH CORRELATED POTENTIAL HARMONICS BASIS

The Hamiltonian for a system of $(N + 1)$ atoms (each of mass m) and interacting via two-body potential has the form

$$H = -\frac{\hbar^2}{2m} \sum_{i=1}^{N+1} \nabla_i^2 + \sum_{i>j=1}^{N+1} V(\vec{x}_i - \vec{x}_j) + \sum_{i>j=1}^{N+1} V_{trap}(\vec{x}_i) \quad (1)$$

where $V(\vec{x}_i - \vec{x}_j) = V(\vec{r}_{ij})$ is the two-body potential described later and \vec{x}_i is the position vector of the i -th particle. We use the standard Jacobi coordinates defined as $\vec{\zeta}_i = \left(\frac{2i}{i+1}\right)^{\frac{1}{2}} \left[\vec{x}_{i+1} - \frac{1}{i} \sum_{j=1}^i \vec{x}_j\right]$, ($i = 1, 2, \dots, N$) and the center of mass through $\vec{R} = \frac{1}{N+1} \sum_{i=1}^{N+1} \vec{x}_i$. Then the relative motion of the atoms is described in terms of N Jacobi vectors $(\vec{\zeta}_1, \dots, \vec{\zeta}_N)$ as [3]

$$\left[-\frac{\hbar^2}{m} \sum_{i=1}^N \nabla_{\vec{\zeta}_i}^2 + V_{trap}(r) + V(\vec{\zeta}_1, \dots, \vec{\zeta}_N) - E \right] \times \Psi(\vec{\zeta}_1, \dots, \vec{\zeta}_N) = 0, \quad (2)$$

where V is the sum of all pair-wise interactions expressed in terms of the Jacobi vectors. We assume that only two-body correlations in the many-body wave function are important [3, 4], This permits the use of the potential harmonics expansion method, in which the total wavefunction Ψ is decomposed into two-body Faddeev components ψ_{ij} for the (ij) interacting pair.

$$\Psi = \sum_{ij>i}^{N+1} \psi_{ij}. \quad (3)$$

Note that with two-body correlations alone, ψ_{ij} is a function only of two-body separation (\vec{r}_{ij}) and a global length, called hyperradius ($r = \sqrt{[\sum_1^N \zeta_i^2]}$) and is independent of the coordinates of all the particles other than the interacting pair [3, 4]. ψ_{ij} (symmetric under P_{ij}) satisfies the Faddeev equation

$$(T + V_{trap} - E)\psi_{ij}(\vec{x}) = -V(\vec{r}_{ij}) \sum_{k,l>k} \psi_{kl}(\vec{x}), \quad (4)$$

T being the total kinetic energy; operating $\sum_{i,j>i}$ on both sides of Eq. (4), we get back the original Schrödinger equation. In this approach we assume that when (ij) pair interacts, the rest of the bosons are inert spectators. Moreover, since particle labels are unimportant, we take \vec{r}_{ij} as $\vec{\zeta}_N$. Next we define a hyperradius $\rho_{ij} = \left[\sum_{k=1}^{N-1} \zeta_k^2\right]^{\frac{1}{2}}$ for the remaining $(N - 1)$ noninteracting bosons[3, 4], such that $\rho_{ij}^2 + r_{ij}^2 = r^2$, $\rho_{ij} = r \sin \phi$ and $r_{ij} = r \cos \phi$. In this choice the hyperspherical coordinates are

$$(r, \Omega_N) = (r, \phi, \vartheta, \varphi, \Omega_{N-1}) \quad (5)$$

where (ϑ, φ) are the two spherical polar angles of the separation vector \vec{r}_{ij} , Ω_{N-1} involves $(3N-4)$ variables: $2(N-1)$ polar angles associated with $(N-1)$ Jacobi vectors $\vec{\zeta}_1, \dots, \vec{\zeta}_{N-1}$ and $(N-2)$ angles defining the relative lengths of these Jacobi vectors [3]. Then the Laplacian in $3N$ -dimensional space has the form

$$\nabla^2 \equiv \sum_{i=1}^N \nabla_{\zeta_i}^2 = \frac{\partial^2}{\partial r^2} + \frac{3N-1}{r} \frac{\partial}{\partial r} + \frac{L^2(\Omega_N)}{r^2}, \quad (6)$$

$L^2(\Omega_N)$ is the grand orbital operator in $D = 3N$ dimensional space. Eigenfunctions of this operator, corresponding to all possible sets of quantum numbers (associated with $3N-1$ degrees of freedom), constitute the complete hyperspherical harmonics (HH) basis. Expansion of Ψ in this basis would lead to an exact treatment. However, the degeneracy of the basis (arising from different allowed values of $3N-1$ quantum numbers for a particular grand orbital quantum number, \mathcal{L}) increases very fast with \mathcal{L} and N . This fact and the fact that calculation of matrix elements involve $(3N-1)$ -dimensional integrals make the calculation extremely cumbersome for $N > 3$. Moreover, imposition of symmetry also becomes very difficult as N increases. Hence the HH expansion method (HHEM) is practicable only for three-body systems. A great deal of simplification is possible for the laboratory BEC, which is extremely dilute and only two-body correlations are important. One can then use a subset [called potential harmonics (PH) basis] of HH basis with great advantage. Potential harmonics for the (ij) -partition are defined as the eigenfunctions of $L^2(\Omega_N)$ corresponding to zero eigenvalue of $L^2(\Omega_{N-1})$. The corresponding eigenvalue equation satisfied by $L^2(\Omega_N)$ is [9]

$$[L^2(\Omega_N) + \mathcal{L}(\mathcal{L} + D - 2)] \mathcal{P}_{2K+l}^{l,m}(\Omega_{ij}) = 0, \quad \mathcal{L} = 2K+l. \quad (7)$$

This new basis is a subset of the full HH set and it does not contain any function of the coordinate $\vec{\zeta}_i$ with $i < N$. It is given by a simple closed expression [9]

$$\mathcal{P}_{2K+l}^{l,m}(\Omega_{ij}) = Y_{lm}(\omega_{ij}) {}^{(N)}P_{2K+l}^{l,0}(\phi) \mathcal{Y}_0(D-3), \quad (8)$$

where $Y_{lm}(\omega_{ij})$ is the spherical harmonics and $\omega_{ij} = (\vartheta, \varphi)$. The function ${}^{(N)}P_{2K+l}^{l,0}(\phi)$ is expressed in terms of Jacobi polynomials [10] and $\mathcal{Y}_0(3N-3)$ is the HH of order zero in the $(3N-3)$ dimensional space, spanned by $\{\vec{\zeta}_1, \dots, \vec{\zeta}_{N-1}\}$ Jacobi vectors [9]. Thus the contribution to the grand orbital quantum number comes only from the interacting pair and the $3N$ dimensional Schrödinger equation reduces effectively to a four dimensional equation. The relevant set of quantum numbers (associated with the hyperangles) are *only three* – orbital l , azimuthal m and grand orbital $2K+l$ for any N . This leads to a dramatic simplification of the many-body calculations. Besides drastic reduction of degeneracy of the basis, potential matrix elements involve only three-dimensional (one-dimensional for central forces) integrals. The physical picture is that all irrelevant degrees of freedom have

been frozen. Using this procedure, we have solved BEC containing up to 14000 bosons [4, 11]. The method has been successfully applied to attractive condensates as well [5, 12–14]. We expand (ij) -Faddeev component, ψ_{ij} , in the complete set of potential harmonics appropriate for the (ij) partition:

$$\psi_{ij} = r^{-(\frac{3N-1}{2})} \sum_K \mathcal{P}_{2K+l}^{lm}(\Omega_N^{(ij)}) u_K^l(r). \quad (9)$$

Note that the notation has been slightly modified to include the superscript (ij) in Ω_N , to indicate that it is the full set of hyperangles in D dimensional space, for the particular choice of Jacobi vector $\vec{\zeta}_N = \vec{r}_{ij}$. Eq. (9) includes two-body correlations only. This is perfectly justified in the context of dilute attractive Bose gas, where the effect of two-body correlation is important and one can safely ignore the effects of higher-body correlations. Taking projection of Eq. (4) on a particular PH, a set of coupled differential equations (CDE) is obtained [3, 4]

$$\begin{aligned} & \left[-\frac{\hbar^2}{m} \frac{d^2}{dr^2} + \frac{\hbar^2}{mr^2} \{ \mathcal{L}(\mathcal{L} + 1) + 4K(K + \alpha + \beta + 1) \} \right. \\ & \left. + V_{trap}(r) - E \right] U_{Kl}(r) \\ & + \sum_{K'} f_{Kl} V_{KK'}(r) f_{K'l} U_{K'l}(r) = 0, \end{aligned} \quad (10)$$

where $U_{Kl}(r) = f_{Kl} u_K^l(r)$, $\mathcal{L} = l + \frac{3N-3}{2}$, $\alpha = \frac{3N-5}{2}$, $\beta = l + \frac{1}{2}$, l being the orbital angular momentum contributed by the interacting pair and K is the hyperangular momentum quantum number. The potential matrix element $V_{KK'}(r)$ is given by [3, 4]

$$V_{KK'}(r) = \int \mathcal{P}_{2K+l}^{lm*}(\Omega_N^{(ij)}) V(x_{ij}) \mathcal{P}_{2K'+l}^{lm}(\Omega_N^{(ij)}) d\Omega_N^{(ij)}. \quad (11)$$

The quantity f_{Kl}^2 is given by

$$f_{Kl}^2 = \sum_{k,l>k} \langle \mathcal{P}_{2K+l}^{lm}(\Omega_N^{(ij)}) | \mathcal{P}_{2K+l}^{lm}(\Omega_N^{(kl)}) \rangle. \quad (12)$$

It is the overlap of the PH for the (ij) -partition (corresponding to only the (ij) -pair interacting) with the sum of PHs for all partitions. An expression for f_{Kl}^2 can be found in Ref [3]. So far we have disregarded the effect of the short range correlation in the PH basis. In the case of a dilute Bose gas, as the energy of the interacting pair is extremely small, the two-body interaction is generally represented by the s -wave scattering length a_{sc} alone (as in the mean-field GP treatment), disregarding its detailed structure. On the other hand, a realistic interatomic potential like the van der Waals interaction has an attractive $-\frac{1}{r_{ij}^6}$ tail at larger separations and a strong repulsion at short separation. The short-range behavior is usually represented by a hard core of radius r_c . For a given two-body potential having a finite range, a_{sc} can be obtained from the asymptotic solution of the zero-energy

two-body Schrödinger equation

$$-\frac{\hbar^2}{m} \frac{1}{r_{ij}^2} \frac{d}{dr_{ij}} \left(r_{ij}^2 \frac{d\eta(r_{ij})}{dr_{ij}} \right) + V(r_{ij})\eta(r_{ij}) = 0. \quad (13)$$

The value of r_c is obtained from the requirement that the calculated a_{sc} has the experimental value. The correlation function quickly attains its asymptotic form ($C_1 + C_2/r_{ij}$) for large r_{ij} . The asymptotic normalization is chosen to make the wavefunction positive at large r_{ij} and the corresponding scattering length is given by $a_{sc} = -\frac{C_2}{C_1}$. In the experimental BEC, the energy of the interacting pair is negligible compared with the depth of the interaction potential. Thus $\eta(r_{ij})$ correctly reproduces the short r_{ij} behavior of $\psi_{ij}(r_{ij}, r)$. Hence we introduce this as a short-range correlation function in the expansion basis and call it as correlated potential harmonics (CPH) basis [5].

$$\left[\mathcal{P}_{2K+l}^{l,m}(\Omega_{(ij)}) \right]_{corr} = Y_{lm}(\omega_{ij}) {}^{(N)}P_{2K+l}^{l,0}(\phi) \times \mathcal{Y}_0(3N-3)\eta(r_{ij}), \quad (14)$$

The correlated potential matrix element $V_{KK'}(r)$ is now given by

$$V_{KK'}(r) = (h_K^{\alpha\beta} h_{K'}^{\alpha\beta})^{-\frac{1}{2}} \int_{-1}^{+1} \left\{ P_K^{\alpha\beta}(z) V \left(r \sqrt{\frac{1+z}{2}} \right) \times P_{K'}^{\alpha\beta}(z) \eta \left(r \sqrt{\frac{1+z}{2}} \right) w_l(z) \right\} dz. \quad (15)$$

Here $h_K^{\alpha\beta}$ and $w_l(z)$ are respectively the norm and weight function of the Jacobi polynomial $P_K^{\alpha\beta}(z)$ [3, 9].

Note that the inclusion of the short-range correlation function, $\eta(r_{ij})$ makes the PH basis non-orthogonal. This introduces an overlap matrix on the eigenvalue side of the matrix eigen value equation. One can use the standard procedure for handling a non-orthogonal basis, by introducing a transformation using the eigenvalues of the overlap matrix to convert the eigenvalue equation into the standard diagonalization of a symmetric matrix. However, we have checked that $\eta(r_{ij})$ differs from a constant value only by a small amount in a relatively small interval. Hence to simplify the calculation, we project Eq. (4) on to a particular PH, *viz.* $\mathcal{P}_{2K+l}^{lm}(\Omega_N^{(ij)})$. The dependence of the overlap $\langle \mathcal{P}_{2K+l}^{lm}(\Omega_N^{(ij)}) | \mathcal{P}_{2K+l}^{lm}(\Omega_N^{(kl)}) \eta(r_{kl}) \rangle$ on the hyperradius r is quite small. Disregarding derivatives of this overlap with respect to the hyperradius, we approximately get back Eq. (10), with $V_{KK'}(r)$ given by Eq. (15).

III. RESULTS

A: CHOICE OF INTERACTION AND CALCULATION OF EFFECTIVE POTENTIAL

We consider the ${}^7\text{Li}$ condensate with $a_{sc} = -27.3$ Bohr. For the numerical calculation, we choose the oscil-

ator units (o.u.) of length and energy, commonly used in BEC calculations. The oscillator length, $a_{ho} = \sqrt{\frac{\hbar}{m\omega}}$ is chosen as the unit of length and the oscillator energy $\hbar\omega$ as the unit of energy, ω being the trapping frequency ($\omega = 2\pi\nu$). However for presenting results, both in tabular form and in figures, we use MKS units: meter (m) and Joule (J) for length and energy respectively. The trap size corresponding to Rice University experiment is $a_{ho} = 3.0\mu\text{m}$. Our chosen potential is the realistic van der Waals potential, which has a strong repulsive core (which is chosen as a hard core of radius r_c) and an attractive tail at larger separations: $V(r_{ij}) = \infty$ for $r_{ij} \leq r_c$ and $= -\frac{C_6}{r_{ij}^6}$ for $r_{ij} > r_c$. The strength (C_6) is known for a given type of atom. In the limit of $C_6 \rightarrow 0$, the potential becomes a hard sphere and r_c coincides with the s -wave scattering length a_{sc} . For the potential including the long range part, a tiny change in r_c may cause an enormous change in a_{sc} , including sign [5]. As r_c decreases from a large value, a_{sc} decreases, and at a particular critical value of r_c , it passes through an infinite discontinuity from $-\infty$ to $+\infty$ [5]. Thereafter the potential supports a two body bound state. This pattern repeats as r_c decreases further. Positive values of a_{sc} correspond to repulsive potential whereas negative a_{sc} values correspond to attractive potential. Thus minute tuning of r_c can cause the effective potential to change from attractive to repulsive. In the mean-field description, the two-body interaction is solely represented by the s -wave scattering length a_{sc} and depending on its sign, positive or negative, the condensate is treated as repulsive or attractive respectively. However in our many-body calculation, we solve zero-energy two-body Schrödinger equation with $V(r_{ij})$ given above and tune r_c to obtain correct value of a_{sc} which mimics the ${}^7\text{Li}$ condensate of Rice University [15]. However with a tiny change in r_c , a_{sc} may change by large amount including the sign. Each additional sign change means that the potential will support an extra two-body bound state and it results in an extra node in $\eta(r_{ij})$. We choose r_c , such that it corresponds to the zero node in the two-body wave function. The chosen parameter for our calculation is $C_6 = 1.71487 \times 10^{-12}$ o.u. and $r_c = 5.3378 \times 10^{-4}$ o.u.. With these sets of parameters we solve the set of coupled differential equations by the hyperspherical adiabatic approximation (HAA) [16]. In HAA, one assumes that the hyperangular motion is slow compared to the hyperangular motion. The effective potential for the hyperradial motion (obtained by diagonalizing the potential matrix together with the diagonal hypercentrifugal repulsion for each value of r) is obtained as a parametric function of r . We choose the lowest eigenpotential ($\omega_0(r)$) as the effective potential. Thus in HAA, energy and wavefunction are obtained approximately by solving a single uncoupled differential equation

$$\left[-\frac{\hbar^2}{m} \frac{d^2}{dr^2} + \omega_0(r) + \sum_{K=0}^{K_{max}} \left| \frac{d\chi_{K0}(r)}{dr} \right|^2 - E \right] \zeta_0(r) = 0, \quad (16)$$

subject to appropriate boundary conditions on $\zeta_0(r)$. The third term is a correction to the lowest order HAA approximation. $\chi_{K0}(r)$ is the K -th component (K being the hyperangular momentum quantum number) of the eigenvector corresponding to the lowest eigenvalue ($\omega_0(r)$) of potential plus hypercentrifugal matrix. This is called uncoupled adiabatic approximation (UAA), whereas disregarding the third term corresponds to the extreme adiabatic approximation (EAA). The principal advantages of the present method are as follows. First, the correlated PH basis keeps all possible two-body correlations and the number of variables is reduced to only four irrespective of the number of bosons in the trap. So by this method, we can treat quite a large number of atoms without much computational difficulty. Second, the use of HAA basically reduces the multidimensional problem to an effective one-dimensional one introducing the effective potential. The effective potential (ω_0) gives clear qualitative as well as quantitative pictures. For our numerical calculation we fix $l = 0$ and truncate the CPH basis to a maximum value $K = K_{max}$, requiring proper convergence. Third, the use of van der Waals interaction with a finite range is more realistic than the use of a zero-range contact interaction, as in the mean-field GP approach. The pathological singularity of the δ -function attractive potential does not arise in the present treatment.

In Fig. 1, we plot the many-body effective potential $\omega_0(r)$ as a function of hyperradius r for $N=200$ atoms in the condensate. As $N = 200$ is less than $N_{cr} \simeq 1300$ [15], the condensate is metastable and is associated with a deep and narrow attractive well (NAW) on the left side. For $r \rightarrow 0$, there is a strong repulsive wall. This is the immediate reflection of using hard core van der Waals interaction. The effective potential for an attractive contact interaction goes rapidly to $-\infty$ as $r \rightarrow 0$, causing an essential and pathological singularity. Thus, our many-body picture with nonlocal interaction is in sharp contrast with the GP mean-field picture with local interaction. The nonlocal interaction and the repulsive core of the van der Waals potential prevent the Hamiltonian from being unbound from below. For N less than the critical value N_{cr} , a metastable region (MSR) appears for larger r , an intermediate barrier (IB) separating the NAW and the MSR. For still larger r , the influence of the attractive interaction subsides and the external wall of the harmonic trap dominates. In panel (a) of Fig. 1, the NAW together with the repulsive core is shown. In panel (b) of the same figure, the IB and MSR have been plotted. The bottom of the NAW has a very large magnitude compared with the bottom of the MSR, hence they cannot be shown in the same figure. Note the widely different scales used in the two panels. Furthermore, r in panel (b) is in logarithmic scale.

With the increase in the number N , we observe

a decrease in the height of the intermediate barrier, together with a decrease in the difference between the maximum of IB and the minimum of MSR and the NAW starts to be more negative and narrower. As $N \rightarrow N_{cr}$, the maximum of IB and the minimum of MSR merge to form a point of inflexion, with the disappearance of the MSR. At $N = N_{cr}$, the metastable condensate collapses. For $N \geq N_{cr}$, there will be only the NAW and no metastable condensate. In our present study we observe the IB just vanishes and the condensate collapses at $N = 1430$. This is the usual collapse of the attractive condensate. At this point, all the atoms get trapped in the NAW and form van der Waals cluster which corresponds to a high-density branch in the density profile.

Next we study different correlation properties in such a realistic condensate. We also investigate how the coherence properties depend on the trap size (a_{ho}) and determine the critical size of the trap.

B : ONE-BODY DENSITY

It was originally pointed out that the BEC is evidenced by the presence of off-diagonal long-range order in the one-particle density matrix [1]. However this definition is not strictly valid in the case of a finite-size inhomogeneous system. Due to the presence of an external harmonic trap, our system is inhomogeneous. In our many-body formalism, we define the one-body density as the probability density of finding a boson at a distance \vec{r}_k from the center of mass of the condensate as

$$R_1(\vec{r}_k) = \int_{\tau'} |\psi|^2 d\tau'. \quad (17)$$

where ψ is the full many-body wave function and the integral over the hypervolume τ' excludes the variable \vec{r}_k . The incremental hypervolume $d\tau'$ is given by

$$d\tau' = r'^{3N-4} \cos^2 \phi \sin^{3N-7} \phi dr' d\phi d\omega_{ij} d\Omega_{N-2} \quad (18)$$

where r' is obtained from the relation

$$r^2 = r'^2 + 2r_k^2 \quad (19)$$

and the other symbols have their usual meanings [17]. The integral is computed analytically followed by numerical computation using a 32-point Gaussian quadrature with the original interval divided into progressively increasing subintervals. According to Penrose and Onsager definition of Bose-Einstein condensation, the one-particle density matrix must be associated with a single macroscopic eigenvalue [1]. However the function $\psi(r)$ can be directly expressed in terms of first-order correlation function [18] and all the information of the one-body density correlation are contained in Eq. (17). The short-range repulsion between interacting atoms

give some new aspects in the atomic correlation. We present our results in Fig. 2 for 200 ${}^7\text{Li}$ atoms with $a_{sc} = -27.3$ Bohr and two different trap sizes: trap frequency $\omega = 1.01$ kHz (corresponding to trap size $a_{ho} = 3.0 \mu\text{m}$) and $\omega = 2.27$ kHz (corresponding to trap size $a_{ho} = 2.0 \mu\text{m}$). The one-body density profile deviates from the Gaussian profile of non-interacting case. For comparison, we include the mean-field GP results. The deviation from the GP result is attributed to the effect of interatomic correlation. For the reduced trap size of $2.0 \mu\text{m}$, we observe that the peak becomes higher and narrower, the difference between the mean-field GP and many-body result also increases, as the system develops shorter range correlations. This can be understood from the fact that in the standard GP approach the NAW is disregarded, which pulls the system inwards. The many-body results for gradually reduced trap sizes are presented in Fig. 3. It was observed earlier that for the homogeneous system the long-range behavior in the one-body density follows a power-law decay [18]. However in the presence of an external trap the long-range tail in the one-body density is of the order of the trap width. Thus by reducing the trap size gradually we observe that the long tail in the one-body density decreases as expected. For a very tight trap, the one-body density is sharply peaked and the long-range order is sharply reduced, in tune with reduced trap size. It indicates that the atoms in the metastable condensate are highly correlated. These features become more clear from Fig. 4, where we plot the change in the MSR of the effective many-body potential with the change in the trap size. In Table I we present the position and the value of the maximum of IB and the second minimum (which comprises the MSR) in the column 3 and 4 respectively. Although the position and the value of the maximum of IB do not change much with the trap size, the position and the value of second minimum are greatly shifted. It indicates that the MSR is pulled in and the condensate shrinks with decrease in trap size. The corresponding interaction energy is presented in column 5 of Table I. With decrease in trap size the attractive interaction energy sharply increases and we find $a_{ho} = 0.42 \mu\text{m}$ as the critical trap size. Just below this critical size the condensate will be destroyed due to high quantum fluctuations as the negative interaction energy increases very fast for smaller a_{ho} . What actually happens is the following. As the trap size is reduced, the system gets squeezed. Consequently, the interatomic spacing reduces and the net attractive interaction energy increases. Eventually, when the interatomic spacing reaches the typical cluster size, tightly bound clusters are formed, together with the complete removal of the metastable condensate. Such a scenario is not possible with an attractive contact interaction, for which the effective potential goes to $-\infty$ as $r \rightarrow 0$. Note that this collapse is different from the usual collapse for $a_{ho} = 3 \mu\text{m}$, where the metastable region vanishes at $N = N_{cr}$. The critical

trap size strongly depends on the number of bosons in the trap, which may be just few tens to a few hundreds depending on the trap frequency. For $N = 200$ atoms the critical trap frequency is $\omega = 51.47$ kHz.

The healing length is sometimes referred to as the coherence length and may be considered a relevant quantity to quantify the correlation in very tight traps. Healing length ζ is basically the minimum distance over which the order parameter can heal. It is in general calculated by balancing the quantum pressure and the interaction energy of the condensate. In Fig. 5 we plot the healing length as a function of the trap size, which shows a steep decrease in ζ in very tight traps. The simple expression for healing length is $\zeta = \frac{1}{\sqrt{8\pi a_{sc} n(0)}}$, where $n(0)$ is the peak density at $r = 0$. However in principle n depends on r and $\zeta(r) = \frac{1}{\sqrt{8\pi a_{sc} n(r)}}$, i.e., as $n(r) \rightarrow 0$, $\zeta(r) \rightarrow \infty$ at the surface of the cloud. We can also compare our results with the simple Gaussian estimate, for which $n(r) = \frac{N}{(\sqrt{\pi} a_{ho})^3} e^{-\frac{r^2}{a_{ho}^2}}$ and $\zeta(0) \simeq a_{ho}^{3/2} \sqrt{8\pi a_{sc} N}$. Thus ζ scales as $a_{ho}^{3/2}$. Thus the smooth decrease of the healing length in Fig. 5 reflects the effect of interatomic interaction and two-body correlation.

As mentioned earlier, in the standard GP mean-field theory, the metastable region vanishes as $N \rightarrow N_{cr}$ and the condensate collapses into the singular well. The fate of the condensate is not predicted further. Here, the many-body picture is different. In our case the narrow attractive well on the left facilitates further study of the condensate near the criticality. The metastable condensate leaks through the intermediate barrier, and settles down in the NAW. The atoms in the condensate form van der Waals clusters via strongly enhanced three- and higher-body collisions. It corresponds to the high-density branch [19]. In Fig. 6 we demonstrate graphically the dependence of the NAW on the trap size. In Table I, we present the position and value of the deep minimum of the NAW in column 1. The position of the deep well and the adjacent barrier, which comprise the NAW, do not change with the trap size. These clearly demonstrate that the high-density branch remains invariant with the trap size. The calculated size of the atomic cluster is of the order of $0.005 \mu\text{m}$.

This high-density stable state within the NAW corresponds to the Li clusters. It would be interesting if these clusters could be detected experimentally. Although there is no experimental study of ${}^7\text{Li}_N$ clusters till now, bosonic ${}^4\text{He}_N$ clusters have been studied experimentally. The size of ${}^4\text{He}$ clusters is determined by the matter wave diffraction gratings [20]. This is a very promising technique for the study of ${}^4\text{He}_N$ clusters. However, such techniques may not be feasible for clusters formed from collapsed BEC, due to small num-

ber of such clusters and difficulty in extracting a beam for the diffraction experiment. Perhaps a better method may be using spectroscopic techniques [21]. Utilizing the Feshbach resonance the effective interaction between two atoms can be changed essentially to any value as desired and it facilitates the creation of large weakly bound clusters. The signature of the universal behavior of weakly bound bosonic cluster is studied in Ref. [22] and can be observed in ultracold Bose gas.

C: PAIR-DISTRIBUTION FUNCTION

So far we have focused on the one-particle density which basically considers analysis of the order parameter and contains all information about the one-particle aspects. In the present section we are interested to calculate the probability $R_2(r_{ij})$ which is defined as the probability of finding the (ij) -pair of particles at a relative separation r_{ij} . For a correlated interacting system we define $R_2(r_{ij})$ as follows

$$R_2(r_{ij}) = \int_{\tau''} |\psi|^2 d\tau'', \quad (20)$$

where ψ is the many-body wavefunction as before but now the integral over the hypervolume τ'' excludes integration over r_{ij} . The incremental hypervolume $d\tau''$ is given by

$$d\tau'' = r_{ij}^2 (r \sin \phi)^{3N-4} d\omega_{ij} d\rho_{ij} d\Omega_{N-1} \quad (21)$$

Our results for the same number of ${}^7\text{Li}$ atoms and for the same trap sizes as in Fig. 3 are presented in Fig. 7. When $R_2(r_{ij})=0$, there is no diagonal correlation. The peak value of R_2 at some distance r_{ij} signifies strong clustering effects. The study of pair correlation is important as the realistic interatomic interaction with a small hard core repulsion plays a crucial role. It forbids the atoms to come *too close* due to nucleus-nucleus repulsion. Thus $R_2(r_{ij})$ is always zero at $r_{ij} = 0$. Unlike the uniform system with no confinement, our calculation shows that R_2 vanishes asymptotically. This is the effect of external confinement which restricts the pair separation to a finite value. In our earlier calculations we observed the dependence of correlation function on the interaction strength [17]. However here we observe that even for weak interaction and just a few hundred atoms, correlation length decreases drastically in a tight trap. To be more quantitative, we define the correlation length as the width of correlation function at the half of its maximum value and plot it as a function of trap size in Fig. 8. In Fig. 8 we also plot the position of clustering spot as a function of trap size. Clustering spot is defined as the position of r_{ij} where pair-distribution function attains a maximum value. Even for such weak interaction, we observe that both the correlation length and position of cluster spot in the metastable condensate decrease drastically, in tune with the trap size, as the trap becomes

tighter. During this squeezing process, the correlation length remains larger than the trap size. It indicates that the metastable condensate remains highly correlated in the tight confinement. But when it is squeezed beyond the critical trap size, clustering of particles occurs with the destruction of metastable BEC.

IV. CONCLUSION

In an attractive BEC, the destruction of the condensate takes place when the number of bosons in the external trap exceeds the critical number. At this point, the interaction energy becomes large negative (so that the kinetic pressure fails to balance it) and the condensate shrinks, such that the density at the center of the trap becomes very high. The ultimate fate is the collapse of the attractive BEC. As the system becomes highly correlated, it is appropriate to undertake a correlated many-body approach to describe several correlation properties of a realistic condensate in a harmonic confinement. The use of a realistic interatomic interaction and the finite size trap give the realistic features in one-body density and pair correlation properties. We calculate such correlation properties of an attractive BEC, using the correlated potential harmonics technique. As the trap size is given by $a_{ho} = \sqrt{\frac{\hbar}{m\omega}}$, it is easy to change the trap size by controlling the laser frequency. A high trapping frequency leads to the creation of a very tight trap. In this report, we undertake the study of correlation properties in a tight trap. Our realistic approach produces an effective potential in which the condensate moves. This effective potential for a metastable condensate has a strongly repulsive core, followed successively by a narrow attractive well, an intermediate barrier, a metastable region in which the metastable condensate resides and finally the high outer wall of the trap. This is in sharp contrast with the mean-field GP approach, for which there is an attractive singularity on the left of the intermediate barrier. The present approach produces a realistic post-collapse scenario. We observe that in a very tight trap, the system becomes highly correlated and effective correlation length is drastically reduced. Even for a small number of atoms well below the critical number, the metastable condensate collapses when the trap size is below a certain value. One can define a critical trap size and critical trap frequency for the existence of a metastable BEC in tight confinement for a given number of atoms with attractive interaction. Below the critical size, the metastable condensate will be destroyed due to high spatial coherence and all the atoms will settle down in the narrow attractive well, with the formation of coherent van der Waals clusters. For small trap sizes above the critical value, the narrow attractive well shows a universal character, becoming independent of the trap size. This shows that the clusters cannot be further squeezed after their formation.

Acknowledgements

AB acknowledges the CSIR, India for a Senior Research Fellowship (Sanction no.: 09/028(0773)/2010-EMR-I).

-
- [1] O. Penrose and L. Onsager, Phys. Rev. A **104**, 576 (1956).
- [2] C. N. Yang, Rev. Mod. Phys. **34**, 694 (1962).
- [3] T.K.Das and B.Chakrabarti, Phys. Rev. A **70**, 063601, (2004).
- [4] T.K.Das, S.Canuto, A.Kundu and B.Chakrabarti, Phys. Rev. A **75**, 042705, (2007).
- [5] T. K. Das, A. Kundu, S. Canuto and B. Chakrabarti, Phys. Lett A **373**, 258 (2009).
- [6] L. Salasnich, Phys. Rev. A **61**, 015601 (1999).
- [7] A. Parola, L. Salasnich and L. Reatto, Phys. Rev. (Rapid Comm.) **57**, R3180 (1998).
- [8] L. Reatto, A. Parola and L. Salasnich, J. Low Temp. Phys. **113**, 195 (1998).
- [9] M.Fabre *de la Ripelle*, Ann. Phys. (N.Y.) **147**, 281, (1983); J.L.Ballot and M.Fabre *de la Ripelle*, Ann. Phys. (N.Y.) **127**, 62, (1980).
- [10] M. Abramowitz and I. A. Stegun, *Handbook of Mathematical Functions*, Dover Publications Inc., New York (1972).
- [11] B. Chakrabarti and T. K. das, Phys. Rev. A **78**, 063608 (2008).
- [12] P. K. Debnath, B. Chakrabarti and T. K. Das, Int. J. Quan. Chem. **111**, 1333 (2011).
- [13] S. K. Haldar, B. Chakrabarti and T. K. Das, Phys. Rev. A **82**, 043616 (2010).
- [14] A. Kundu, B. Chakrabarti, T. K. Das and S. Canuto, J. Phys. B **40**, 2225 (2007).
- [15] C. C. Bradley, C. A. Sackett and R.G. Hulet, Phys. Rev. Lett. **78**, 985 (1997).
- [16] T.K.Das, H.T.Coelho and M.Fabre *de la Ripelle*, Phys. Rev. C **26**, 2288, (1982).
- [17] A. Biswas, B. Chakrabarti and T. K. Das J. Chem. Phys. **133**, 104502 (2010).
- [18] M. Naraschewski and R.J.Glauber, Phys. Rev. A **59**, 4595 (1999)
- [19] A. Biswas, T. K. Das, L. Salasnich and B. Chakrabarti Phys. Rev. A **82**, 043607 (2010).
- [20] R. Brühl *et al*, Phys. Rev. Lett. **95**, 063002 (2005).
- [21] Y. Xu and W. Jäger, Phys. Chem. Chem. Phys. **2**, 3549 (2000).
- [22] G. J. Hanna and D. Blume, Phys. Rev. A **74**, 063604 (2006).

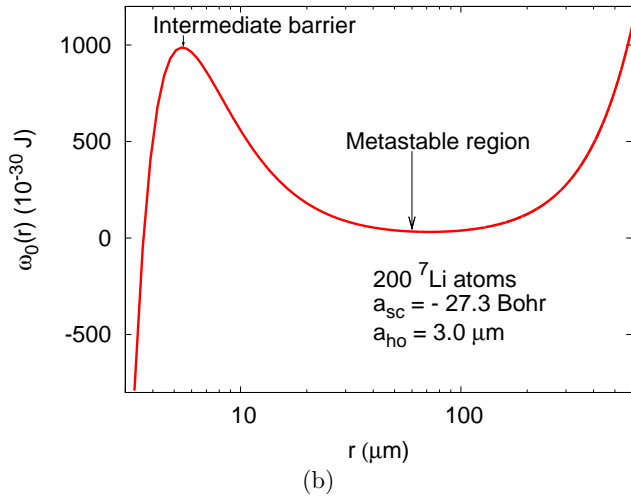
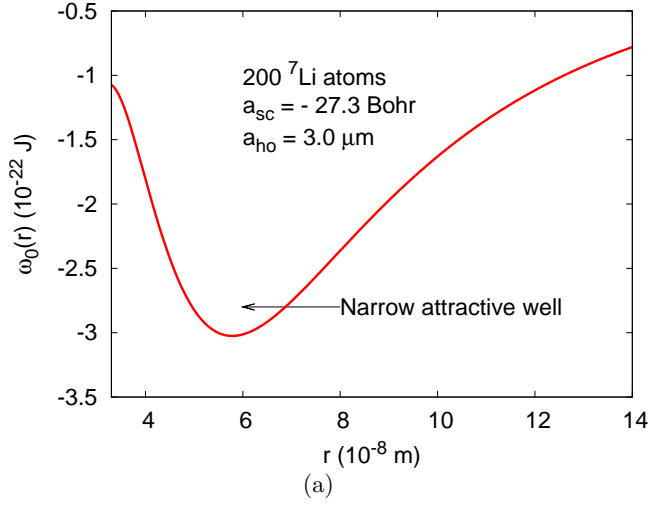


FIG. 1. (Color online) Plot of the effective potential $\omega_0(r)$ against r for 200 ${}^7\text{Li}$ atoms in the usual trap of size $a_{\text{ho}} = 3.0 \mu\text{m}$. The upper panel shows the narrow attractive well (NAW). The lower panel shows the metastable region separated from NAW by the intermediate barrier (IB). Note the different scales used for r and $\omega_0(r)$ in the two panels, so that NAW is far to the left of the plot in panel (b) in which r is in logarithmic scale. Therefore, the NAW is not visible in panel (b). Note also that the bottom of the NAW would have a value $\approx -3 \times 10^8$ in the unit used in panel (b).

TABLE I. Parameters for NAW, IB and MSR of the effective potential and the interaction energy $\langle V \rangle$ for different trap sizes. r_i and ω_i correspond to the position and value of the extrema of NAW ($i = 1$), IB ($i = 2$) and MSR ($i = 3$). Note that different units have been used in different columns.

a_{ho} (μm)	NAW		IB		MSR		$\langle V \rangle$ ($10^{-30} J$)
	r_1 (10^{-8}m)	ω_1 ($10^{-22} J$)	r_2 (μm)	ω_2 ($10^{-28} J$)	r_3 (μm)	ω_3 ($10^{-28} J$)	
3.0	5.79	-2.93	5.40	9.56	71.70	0.31	-0.861
2.0	5.78	-2.92	5.40	9.54	47.40	0.68	-2.915
1.0	5.80	-2.92	5.50	9.61	22.80	2.61	-26.127
0.5	5.80	-2.92	5.70	10.72	10.05	9.22	-306.84
0.42	5.80	-2.92	6.47	12.11	7.22	12.09	-1321.94

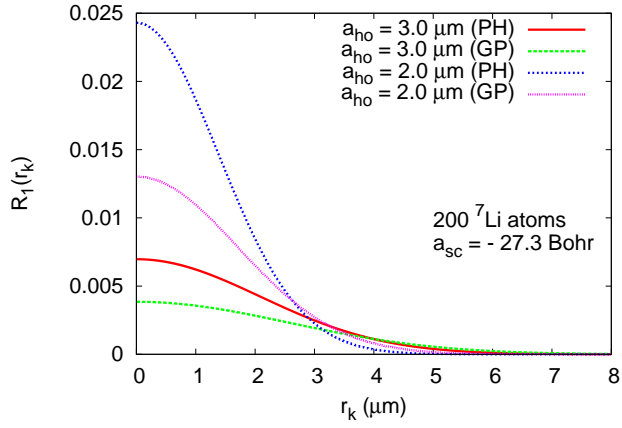


FIG. 2. (Color online) Plot of one-body density ($R_1(r_k)$) against r_k for 200 ${}^7\text{Li}$ atoms in the trap with the size of 3.0 μm and 2.0 μm . Comparison with the mean field GP results is also presented.

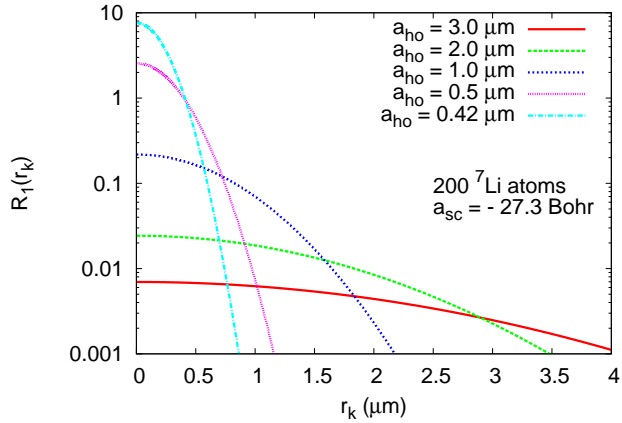


FIG. 3. (Color online) Plot of one-body density ($R_1(r_k)$) against r_k for the same number of atoms as before with different trap sizes.

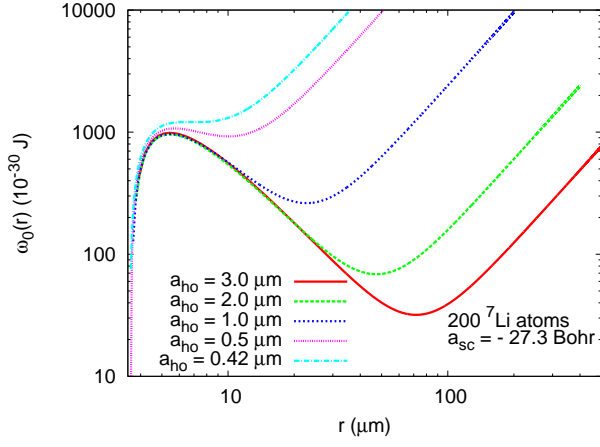


FIG. 4. (Color online) Change in the position and the depth of metastable region for 200 atoms with different trap sizes.

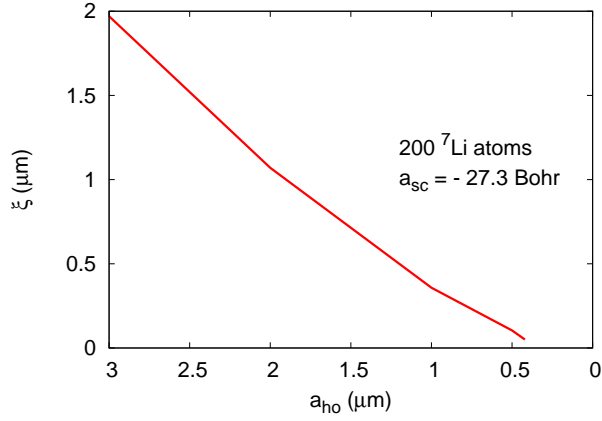


FIG. 5. (Color online) Plot of healing length as a function of trap size.

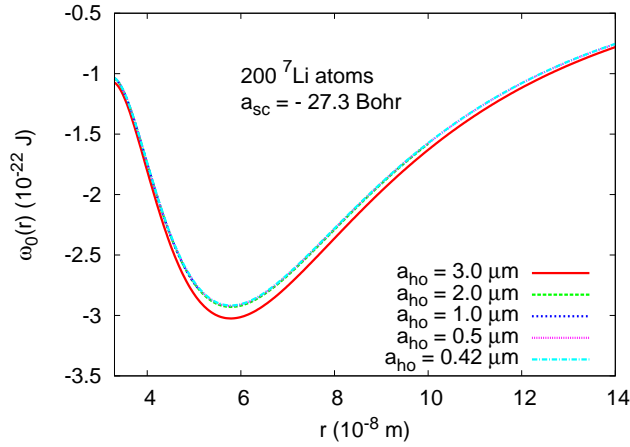


FIG. 6. (Color online) Plot of narrow attractive well for various trap sizes.

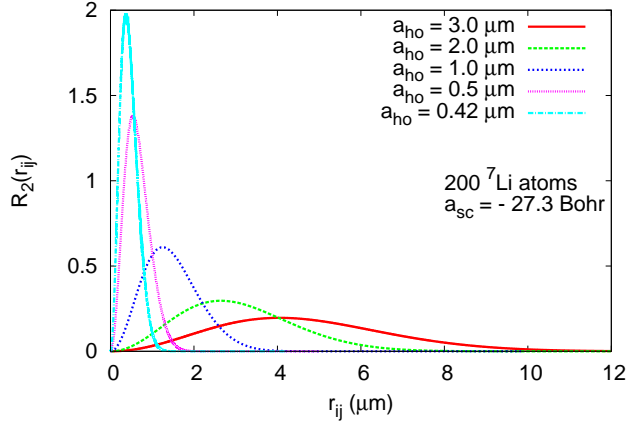


FIG. 7. (Color online) Plot of pair distribution function ($R_2(r_{ij})$) against r_{ij} for an attractive Bose gas with different trap sizes.

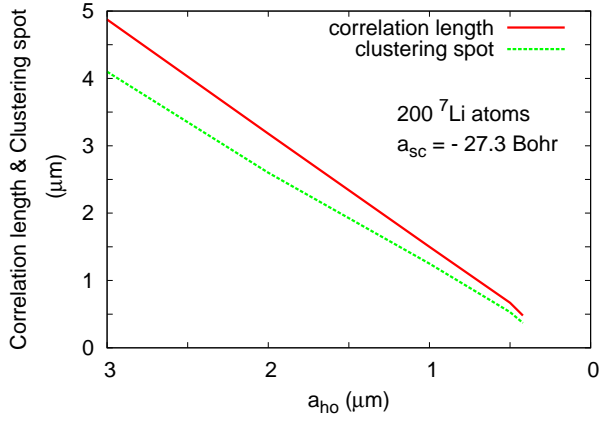


FIG. 8. (Color online) Plot of correlation length and clustering spot as a function of trap size.